Designing of π-phase-shifted fibre Bragg grating with the limit linewidth of the transmission peak

WEN-QING MAN*, CHENG-YUN ZHANG, JUN PENG, QING-PING HE
School of Physics and Materials Science, Guangzhou University, Guangzhou 510006, PR China

The π-phase-shifted fibre Bragg gratings (π-PS-FBG) with the limit linewidth of the transmission peak is numerically investigated and designed. The investigation is divided into two scenarios. In the first scenario, the length of π-PS-FBG is 25 mm, when the index change of π-PS-FBG increases from 1.8×10^{-4} to 5.4×10^{-4}, the linewidth of the transmission peak of π-PS-FBG decreases from 2 MHz to 0.17 Hz. In the second scenario, the index change of π-PS-FBG is 2×10^{-3}, when the length of π-PS-FBG increases from 3 mm to 6.8 mm, the linewidth of the transmission peak of π-PS-FBG decreases from 1.2 MHz to 0.56 Hz. The numerical results indicate that the limit linewidth of the transmission peak of the designed π-PS-FBG is 0.17 Hz and 0.56 Hz, respectively.

(Received May 9, 2023; accepted April 15, 2025)

Keywords: Phase-shifted fibre Bragg gratings, Limit linewidth, Transmission peak

1. Introduction

Fibre Bragg Grating (FBG) was reported by Hill and co-workers in 1978 [1]. FBG contains a phase shift at its center, commonly called phase-shifted FBG (PS-FBG). The PS-FBG has a very sharp transmission peak in the transmission spectrum [2, 3], and due to this advantage, the PS-FBG can be used as a narrow linewidth filter in optical fibre communication [4, 5] or used as a high-resolution optical fibre sensor [6-11]. The PS-FBG is often used to accomplish a narrow linewidth fibre laser [12-16] or to reduce the linewidth of the laser diode [17, 18]. The narrow linewidth laser can be used in coherent optical communication, high-resolution spectral measurement, etc. [16]. When the linewidth of the laser reaches hertz-level [19-21], it can be used in optical atomic clocks and optical frequency combs. The PS-FBG with the limit linewidth transmission peak can be used to reduce the linewidth of the laser to hertz-level.

The PS-FBG can be inscribed in a fibre using a phase mask and UV light. In general, the index change of the PS-FBG ranges from 10^{-5} to 10^{-4}. The length of the PS-FBG is several centimeters. For example, the index change of the PS-FBG is 1.5×10^{-4}, the length of the PS-FBG is 25 mm, and the line width of the transmission peak is 10 pm [7]. In this paper, the index change of the PS-FBG refers to the depth of refractive index modulation of the PS-FBG, the same is true for the rest of the paper.

Although there has been extensive research on the PS-FBG, the PS-FBG with kHz or Hz level linewidth of the transmission peak reported in experimental research is not common. Two PS-FBGs with an ultra-narrow linewidth of the transmission peak were fabricated with a phase mask and UV light in 2010, the linewidth of the transmission peak of the PS-FBG is 15 MHz and 9 MHz, respectively [17,18].

Increasing the length and index change of FBG enhances the reflectivity of FBG [22]. FBG is written in fibre using hydrogen loading technology to increase the index change of FBG, and the index change of FBG can be as high as 5.9×10^{-3} [23]. FBG and PS-FBG can be fabricated using a femtosecond laser and phase mask [24-28] or written with a point-by-point method using a femtosecond laser [29-31]. The index change of FBG written with a femtosecond laser can reach 6×10^{-3} even in standard telecommunication fibre [32-34]. FBGs with extremely high reflectivity have been used to build high-finesse resonant cavities, the reflectivity of FBGs can reach as high as 99.9% [35, 36]. All these developed techniques will enable the researcher to fabricate the PS-FBG with an ultra-narrow linewidth of the transmission peak.

The numerical investigation and designing of π-PS-FBG with the limit linewidth of the transmission peak is presented in this paper. The principle of the limit linewidth of the transmission peak of π-PS-FBG is shown in Section 2, the numerical investigation and designing of two π-PS-FBGs with the limit linewidth of the transmission peak are shown in Section 3 and Section 4, and the conclusion is shown in Sections 5.

2. Principle of the limit linewidth of π-PS-FBG

The schematic diagram of π-PS-FBG is depicted in Fig. 1. Although π-PS-FBG is a non-uniform fibre grating, it can be divided into uniform fibre gratings FBG1, FBG2, and π phase shift. At the input side of π-PS-FBG, the amplitudes

of the forward and backward propagating waves are R_0 and S_0. At the output side of π-PS-FBG, the light amplitudes are R_M and S_M. Then the well-known transmission matrix method is used to investigate its properties [22].

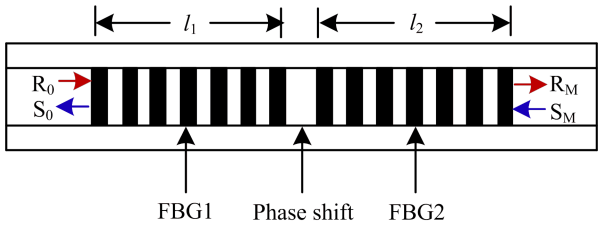

Fig. 1. Schematic diagram of π-PS-FBG (colour online)

For simplicity and practical application, π-PS-FBG is generally made of two identical FBGs and a π phase shift, that is, FBG1 and FBG2 have the same length and index modulation. FBG1 and FBG2 were named FBG later in the paper. In such a particular case, the analytical expression of the transmission spectrum and the linewidth of π-PS-FBG can be derived.

The reflectivity of π-PS-FBG is written as:

$$R = \left|\frac{S_0}{R_0}\right|^2 = \left|\frac{F_{21}}{F_{22}}\right|^2 = \frac{4k^2\hat{\sigma}^2 sinh^4(\gamma_B l)}{(\hat{\sigma}^2 - k^2)^2} \tag{1}$$

where, $\gamma_B = \sqrt{k^2 - \hat{\sigma}^2}$, k is the coupling coefficient, $k = \frac{\pi\delta n_{eff}}{\lambda_B}$, δn_{eff} is the index change of FBG; l represents the length of FBG, that is $l_1 = l_2 = l$; $\hat{\sigma}$ is "dc" self-coupling coefficient, since FBG is a weakly modulated uniform fibre grating, therefore, $\hat{\sigma}$ is approximated as: $\hat{\sigma} = \delta$; δ is the Bragg wavelength detuning of FBG, and $\delta = 2\pi n_{eff}\,(1/\lambda - 1/\lambda_B)$, n_{eff} is the effective index of the fibre core mode LP01.

When the amplitude of the transmission peak of π-PS-FBG equals 0.5, δ represents the linewidth of the transmission peak of π-PS-FBG. From formula (1), the linewidth of the transmission peak of π-PS-FBG is derived as:

$$\begin{aligned}\delta_{peak} &= k\left|\sqrt{2sinh^4(kl)+1} - \sqrt{2}sinh^2(kl)\right| \\ &\approx k/\left[\sqrt{2}cosh(2kl) - \sqrt{2}\right]\end{aligned} \tag{2}$$

For a large value of kl, δ_{peak} is approximated as:

$$\delta_{peak} \approx \sqrt{2}k/e^{2kl} \tag{3}$$

where, $k = \frac{\pi\delta n_{eff}}{\lambda_B}$.

From formula (3), it can be found that the linewidth of the transmission peak of π-PS-FBG is positively proportional to the index change of FBG δn_{eff} and inversely proportional to $e^{\frac{2\pi\delta n_{eff}}{\lambda_B}\cdot l}$.

According to the mathematical property, $e^{\frac{2\pi\delta n_{eff}}{\lambda_B}\cdot l}$ grows faster than δn_{eff}, as a result, the linewidth of the transmission peak significantly decreases as the index change or length of FBG increases. When the index change or length of FBG reaches an appropriate value, the limit linewidth of the transmission peak of π-PS-FBG is achieved, which is the aim of this work.

3. Limit linewidth of the transmission peak of the π-PS-FBG when its length is 25 mm

Suppose that π-PS-FBG is fabricated in the standard single mode fibre with the commercial phase mask. The length of π-PS-FBG is 25 mm, the length of FBG1 (or FBG2) is half that of π-PS-FBG, namely, 2.5 mm. The index of the fibre core mode LP01 is 1.4486, and the index change of π-PS-FBG ranges from 1.8×10^{-4} to 5.4×10^{-4}.

For clarity, the parameters of π-PS-FBG are listed in Table 1.

Table 1. Parameters of π-PS-FBG

Parameter	Symbol	Value
Effective index of the fibre core mode LP01	n_{eff}	1.4486
Index change of π-PS-FBG	δn_{eff}	From 1.8×10^{-4} to 5.4×10^{-4}
Phase shift		π
Bragg wavelength of FBG	λ_B	1550 nm
Period of FBG	Λ	535nm
Length of π-PS-FBG	L	25 mm

The numerical results are shown in Fig. 2, the linewidth of the transmission peak of π-PS-FBG significantly decreases as its index change increases. When the index change of π-PS-FBG increases from 1.8×10^{-4} to 5.4×10^{-4}, the linewidth of the transmission peak of π-PS-FBG decreases from 2 MHz to 0.17 Hz. It should be noted that the amplitude of the transmission peak of all π-PS-FBG are 100% within this range.

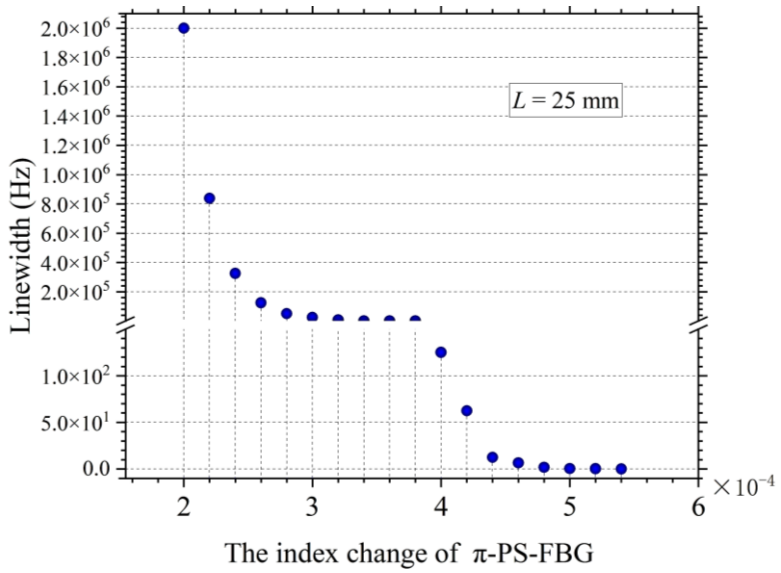

Fig. 2. Linewidth of the transmission peak of π-PS-FBG decreases as its index change increases (colour online)

When the index change of π-PS-FBG is 5.4×10^{-4}, the linewidth of the transmission peak of π-PS-FBG is 0.17 Hz, this is the limit linewidth of the transmission peak of π-PS-FBG. The calculated transmission peak of π-PS-FBG is shown in Fig. 3.

Furthermore, when the index change of π-PS-FBG is 5.6×10^{-4}, 5.8×10^{-4}, and 6.2×10^{-4} respectively, although the linewidth of the transmission peak of π-PS-FBG continues to decrease, the amplitude of the transmission peak begins to decline, it is 98%, 85% and 43%, correspondingly. In short, when the index change of the π-PS-FBG exceeds 5.4×10^{-4}, the amplitude of the transmission peak of π-PS-FBG gradually decreases, and the transmission peak eventually disappears. This is because that the reflectivity of FBG1 and FBG2 approaches to 1 when the index change of π-PS-FBG exceeds a specific threshold, few or no light waves can propagate through the stopband of FBG.

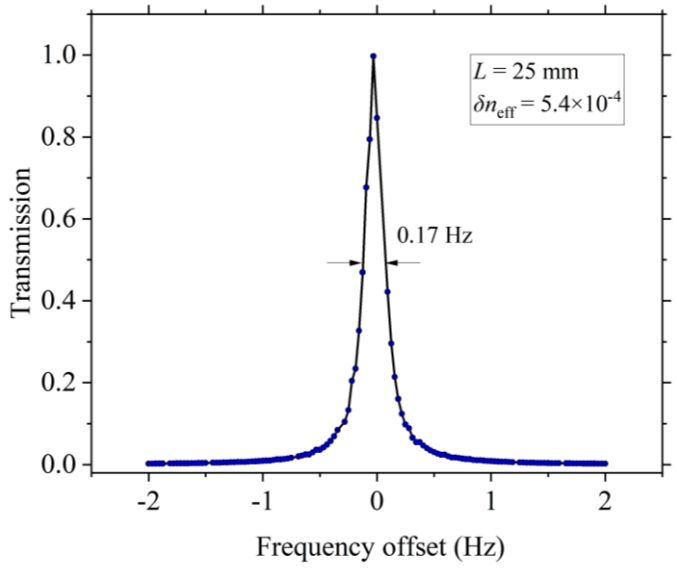

Fig. 3. Transmission peak of π-PS-FBG, the linewidth is 0.17 Hz (colour online)

4. Limit linewidth of the transmission peak of the π-PS-FBG when its index change is 2×10^{-3}

In this section, π-PS-FBG with higher index change is designed. The index change of π-PS-FBG reaches 2×10^{-3}, which can be achieved by a femtosecond laser [32]. The other parameters of π-PS-FBG are the same as the parameters in Table 1, the calculated results are shown in Fig. 4. When the length of π-PS-FBG increases from 3 mm to 6.8 mm, the linewidth of the transmission peak of π-PS-FBG decreases from 1.2 MHz to 0.56 Hz, the amplitude of the transmission peak of all π-PS-FBG are 100% within this range.

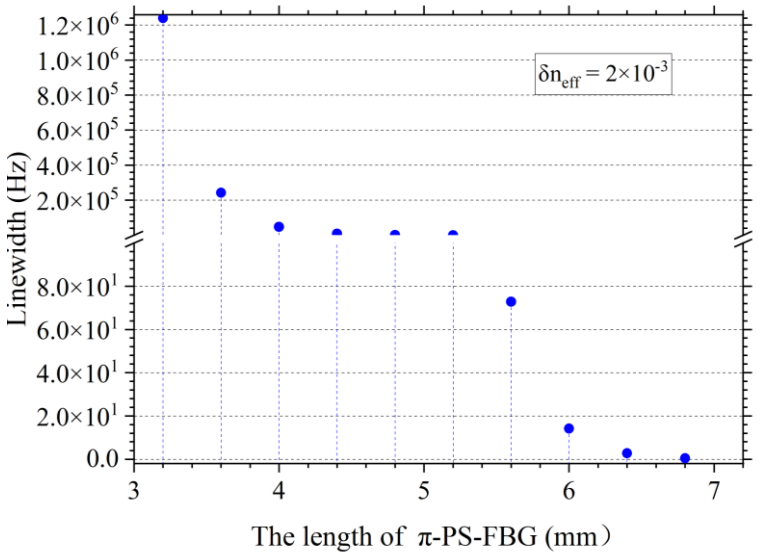

Fig. 4. Linewidth of the transmission peak of π-PS-FBG decreases as its length increases (colour online)

When the length of π-PS-FBG is 6.8 mm, the linewidth of the transmission peak of π-PS-FBG is 0.56 Hz, this is the limit linewidth of π-PS-FBG. The calculated transmission peak of π-PS-FBG is shown in Fig. 5.

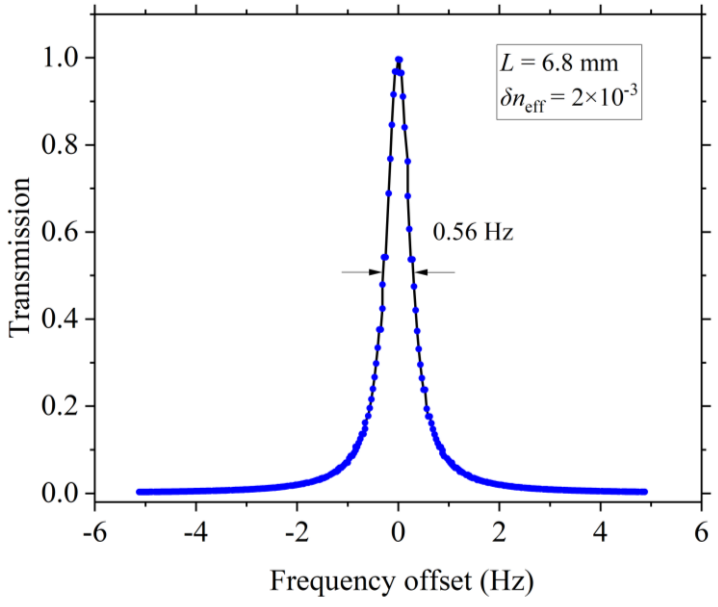

Fig. 5. Transmission peak of π-PS-FBG, the linewidth is 0.56 Hz (colour online)

When the length of π-PS-FBG exceeds 7.2 mm, the reflectivity of FBG1 and FBG2 approaches 1. This feature is similar to that of FBG1 and FBG2 within the π-PS-FBG discussed in Section 3. Under such conditions, few or no light waves can propagate through the stopband of FBG. As a result, the amplitude of the transmission peak of π-PS-FBG gradually decreases, and the transmission peak eventually disappears.

5. Conclusion

The π-phase-shifted fibre Bragg gratings with limit linewidth of the transmission peak is numerically investigated and designed. The limit linewidth of the two π-PS-FBG can reach sub-hertz levels. The first π-PS-FBG has a length of 25 mm, when the index change of π-PS-FBG is 5.4×10^{-4}, the limit linewidth of the transmission peak is reduced to 0.17Hz. The second π-PS-FBG has an index change of 2×10^{-3}, when the length of π-PS-FBG reaches 6.8 mm, the limit linewidth of the transmission peak is reduced to 0.56 Hz. In comparison, the linewidth of the transmission peak of π-PS-FBG reported in experimental research is 9MHz [18]. Therefore, the linewidth of the transmission peak of the π-PS-FBG designed in this study is reduced by seven orders of magnitude.

The calculated results indicate that the linewidth of the transmission peak of π-PS-FBG can reach sub-hertz levels, and the linewidth is significantly affected by the index change for a given length of π-PS-FBG. These results mean that the challenges in the fabrication of π-PS-FBG with the limit linewidth of the transmission peak lie in precisely achieving the index change of π-PS-FBG. In addition, the measurement of the limit linewidth of the transmission peak requires high-resolution measuring instruments.

Acknowledgments

This work was supported by the National Natural Science Foundation of China (No. 11974085).

References

[1] K. O. Hill, Y. Fujii, D. C. Johnson, B. S. Kawasaki, Applied Physics Letters **32**, 647 (1978).
[2] J. Canning, M. G. Sceats, Electronics Letters **30**, 1344 (1994).
[3] R. Kashyap, P. F. Mckee, D. Armes, Electronics Letters **30**, 1977 (1994).
[4] G. P. Agrawal, S. Radic, IEEE Photonics Technology Letters **6**, 995 (1994).
[5] M. Li, H. Li, Y. Painchaud, Optics Express **16**, 19388 (2008).
[6] A. Rosenthal, D. Razansky, V. Ntziachristos, Optics Letters **36**, 1833 (2011).
[7] D. Gatti, G. Galzerano, D. Janner, S. Longhi, Optics Express **16**, 1945 (2008).
[8] R. Wang, Q. Wu, K. Xiong, J. Ji, H. Zhang, H. Zhai, IEEE Sensors Journal **19**, 9790 (2019).
[9] K. S. Jasjot, G. Neena, D. Divya, Optical Engineering **59**, 060901 (2020).
[10] L. Ji, G. Li, C. Zhang, J. Su, C. Wu, IEEE Sensors Journal **21**, 27482 (2021).
[11] Zh. Xie, J. Li, D. Guo, W. Xia, H. Yan, M. Wang, Optics and Laser Technology **172**, 110496 (2024).
[12] W. H. Loh, R. I. Laming, Electronics Letters **31**, 1440 (1995).
[13] M. Jing, B. Yu, J. Hu, H. Hou, G. Zhang, L. Xiao, S. Jia, Scientific Reports **7**, 1895 (2017)
[14] M. I. Skvortsov, A. A. Wolf, A. A. Vlasov, K. V. Proskurina, A. V. Dostovalov, O. N. Sverchkov, B. I. Benker, S. L. Semjonov, S. A. Babin, Scientific Reports **10**, 14487 (2020).
[15] Q. Wen, F. Zhu, Optics Express **29**, 43679 (2021).
[16] Z. Bai, Z. Zhao, M. Tian, D. Jin, Y. Pang, S. Li, X. Yan, Y. Wang, Z. Lu, Microwave and Optical Technology Letters **64**, 2244 (2022).
[17] M. Poulin, Y. Painchaud, S. Ayotte, C. Latrasse, G. Broucu, F. Pelletier, M. Morin, M. Guy, J.-F. Cliché, Proc. SPIE **7579**, 75791C (2010).
[18] Y. Painchaud, M. Aubé, G. Brochu, M. Picard, in proceedings of Advanced Photonics & Renewable Energy Conference (2010), OSA Technical Digest (CD), paper BTuC3.
[19] S. Gundavarapu, G. M. Brodnik, M. Puckett, T. Huffman, D. Bose, R. Behunin, J. Wu, T. Qiu, C. Pinho, N. Chauhan, J. Nohava, P. T. Rakich, K. D. Nelson, M. Salit, D. J. Blumenthal, Nature Photonics **13**(1), 60 (2019).
[20] W. Jin, Q.-F. Yang, L. Chang, B. Shen, Nature Photonics **15**(5), 346 (2021).
[21] W. Liang, Y. Liu, Optics Letters **48**, 1323 (2023).
[22] T. Erdogan, Journal of Lightwave Technology **15**, 1277 (1997).
[23] P. J. Lemaire, R. M. Atkins, V. Mizrahi, W. A. Reed, Electronics Letters **29**, 1191 (1993).
[24] S. J. Mihailov, C. W. Smelser, P. Lu, R. B. Walker, D. Grobnic, H. Ding, G. Henderson, J. Unruh, Optics Letters **28**(12), 995 (2003).
[25] J. He, Y. Wang, C. Liao, Q. Wang, K. Yang, B. Sun, G. Yin, S. Liu, J. Zhou, J. Zhao, Optics Letters **40**(9), 2008 (2015).
[26] A. Halstuch, A. A. Ishaaya, Optical Fibre Technology **67**, 102689 (2021).
[27] A. Ioannou, K. Kalli, Optics Letters **48**, 1826 (2023).
[28] A. Halstuch, A. A. Ishaaya, Optics and Lasers in Engineering **160**, 107286 (2023).
[29] X. Zhou, Y. T. Dai, J. M. Karanja, F. F. Liu, M. H. Yang, Optical Engineering **56**, 027108 (2017)
[30] Y. Sun, Y. Yao, H. Niu, H. Zha, L. Zhang, Z. Tian,

N.-K. Chen, Y. Ren, Optics Communications **521**, 128583 (2022).
[31] X. Y. Sun, L. Zeng, H. F. Du, X.R. Dong, Z. K. Chang, Y. W. Hu, J. A. Duan, Optics and Laser Technology **124**,105969 (2020).
[32] E. Fertein, C. Przygodzk, H. Delbarre, A. Hidayat, Applied Optics **40**, 3506 (2001).
[33] R. Gattass, E. Mazur, Nature Photonics **2**, 219 (2008).
[34] J. W. Zhang, Q. Zhao, D. W. Du, Y. X. Zhu, S. N. Zheng, D.Y. Chen, J. L. Cui, Materials Today Communications **39**, 108760 (2024).
[35] J. Albert, A. Schülzgen, V. L. Temyanko, S. Honkanen, N. Peyghambarian, Applied Physics Letters **89**, 101127 (2006).
[36] S. Kato, T. Aoki, Physical Review Letters **115**, 093603 (2015).

*Corresponding author: lxy_mwq@gzhu.edu.cn